Diode Laser Spectroscopy of Ammonia and Ethylene Overtones

A. Lucchesini *, S. Gozzini

Istituto per i Processi Chimico-Fisici del CNR
Area della Ricerca - Via G. Moruzzi, 1 - I-56124 Pisa - Italy

Abstract

Some overtone absorption lines of ammonia and ethylene have been examined by using a tunable diode laser (TDL) spectrometer in the region around 12650 and 11800 cm^{-1} respectively. The spectrometer sources are commercially available double heterostructure InGaAlAs and AlGaAs TDLs operating in the "free-running" mode. The high resolving power ($\sim 10^7$) of the spectrometer permitted the detection and the study of the line positions of such molecules with a precision better than 0.01 cm^{-1}. In order to maximize the signal to noise ratio and to extract the necessary informations either on the line width and on the line position for the detected molecular resonances, the wavelength modulation spectroscopy (WMS) along with the 2nd harmonic detection techniques have been applied. For this purpose the fitting procedure took into account the instrumental effects and the amplitude modulation (AM) always associated with the frequency modulation (FM) of these type of sources. This technique permitted also the measurement of the collisional broadening and shifting coefficients by different buffer gases at room temperature.

Key words: Overtone absorption spectroscopy, Tunable diode-laser spectrometer, Line widths and shapes, Pressure broadening coefficients

1 Introduction

The availability of tunable laser sources, like commercial diode lasers (DLs), increases the interest on the spectroscopy of overtone and combination bands in the visible (VIS) and in the near-infrared (NIR). DLs are suitable radiation sources for high resolution spectroscopy in the "free-running" mode and

---

* Corresponding author. Fax: +39 0503152-230
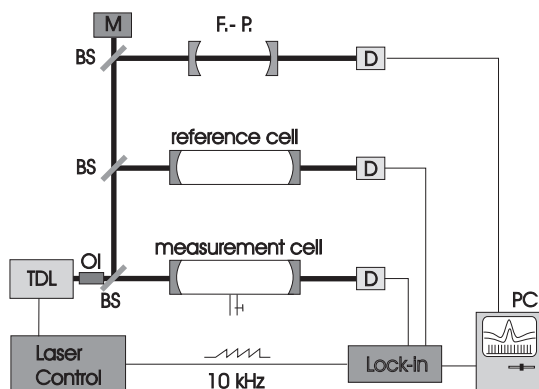 *Email address:* `lucchesini@ipcf.cnr.it` (A. Lucchesini).

Fig. 1. Outline of the experimental apparatus. BS: beam splitter; D: photodiode; F.-P.: Fabry-Perot interferometer; M: monochromator; OI: optical insulator; TDL: tunable diode laser.

in particular for the study of the optical resonances of many molecules, like CH_4 [1], C_2H_2 [2], C_2H_4 [3,4], CHF_3 [5], CO [6], CO_2 [7,8], HF [9], HCl [10], H_2O [11], H_2S [8], HCN [12], NH_3 [13], NO [14], NO_2 [15,16], O_2 [17], etc. ... (the quoted references do not represent an exhaustive list for each species). They can be easily modulated through their injection current, allowing the use of frequency modulation (FM) techniques. By this way high sensitivity tunable diode laser (TDL) spectrometers have been made to monitor trace species even at atmospheric pressure [18]. When the amplitude of the FM is chosen much lower than the resonance line-width, the FM spectroscopy is usually called wavelength modulation spectroscopy (WMS).

Here we apply WMS and second harmonic detection to ammonia and ethylene in the VIS and NIR range in order to detect these species in various atmospheric environments and to determine the spectroscopic line parameters. Besides their presence in the earth environment, these gases are also atmospheric constituents of the outer planets, therefore a knowledge of their absorption pressure-broadening coefficients is helpful for remote sensing the atmospheres of these planets.

The laser sources adopted for this purpose are low-cost commercial type double heterostructure cw DLs working at room temperature (RT).

2 Experimental setup

Fig. 1 shows the experimental arrangement used for the WMS. The source is a Fabry-Perot type semiconductor laser without any external optical feedback, i.e. it operates *free-running*. It is driven by a stabilized low-noise current supply. Its temperature is monitored by a high-stability controller ($\Delta T = 0.01$ K within 1 hour). The temperature control of the DL is very important as its

emission wavelength is a linear function of the temperature with a slope of about 0.1 nm/K. The wavelength scan is obtained by adding a low frequency (~ 1 Hz) sawtooth signal to the driving current. The wavelength dependence on the current is linear (≈ 0.01 nm/mA) for small current variations and is a critical parameter for "free-running" DL spectroscopy (usual current modulation amplitude of ~ 10 mA). The collimated DL radiation is split in three different beams, which go through a confocal 5 cm Fabry-Perot interferometer to check the frequency sweep and the laser emission mode, and through two different glass cells containing the sample gas: one at a constant pressure as reference, and the other at progressively increased pressure. The transmitted radiation is collected by silicon photodiodes and the resulting signals are simultaneously acquired by a desk-top computer. A 35 cm focal length monochromator was employed for the rough wavelength reading($\Delta\lambda \simeq 0.01$ nm). For the harmonic detection a sinusoidal current is mixed to the diode laser injection current: the signals transmitted through the two cells are sent to a lock-in amplifier to extract the desired harmonic component. An optical insulator was put in front of the DL in order to avoid increased noise due to the feedback coming from reflections on the various optical elements along the different beams.

2.1 Frequency modulation technique

When FM is used, the emission frequency of the DL is sinusoidally modulated via the injection current,

$$\nu = \bar{\nu} + m\cos 2\pi\nu_m t \tag{1}$$

and the n-th harmonic component of the transmitted signal is detected by a lock-in amplifier at a reference frequency $n\nu_m$, multiple of the modulation frequency. When the amplitude m of the modulation is small compared to the width of the absorption line, the n-th harmonic component is proportional to the n-th derivative of the transmitted signal. In our work usually we limited $m \ll \Gamma_G$, the Gaussian half width at half the maximum (HWHM), and we detected the second harmonic component ($2f$ detection).

When modulating the DL emission frequency, the presence of a residual amplitude modulation (RAM), even if relatively small, produces a sloping background in the direct absorption (DA) signal and an asymmetry in the $2f$ signal. As shown in Fig. 2, the center of the line does not match the maximum of the $2f$ signal. The displacement is proportional to the slope of the emission profile as well as to the width of the line. This issue is of prime importance for determining the pressure induced shift, since the apparent displacement of the center is proportional to the pressure, as shown in the following discussions.
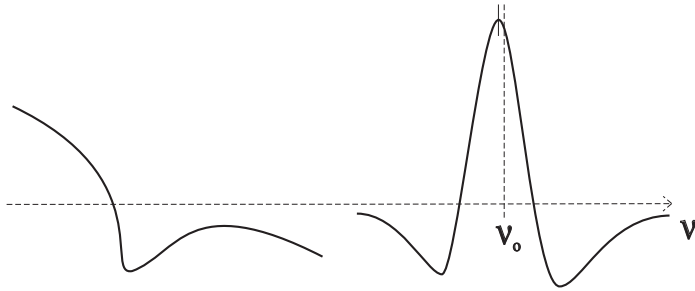
Fig. 2. DA (left) and 2nd harmonic WM signal (right) as detected by the DL spectrometer.

Generally the intensity of the radiation transmitted through a sample can be written as the product of the incoming intensity $I_0(\nu)$ and the transmittance $T(\nu)$, where ν is the distance from the central frequency of the line:

$$I(\nu) = I_0(\nu)T(\nu) \, . \tag{2}$$

The transmittance can be described by the Lambert-Beer equation:

$$T(\nu) = e^{-\sigma(\nu)\,x} \, , \tag{3}$$

where $x = \rho\,l$ is the column amount (in molecule $\cdot$ cm^{-2}), i.e. the product of the absorbing species number density (in molecule $\cdot$ cm^{-3}) and the optical path l (in cm) of the radiation through the sample; the absorption cross section $\sigma(\nu)$ is expressed in cm^2/molecule. In case of small optical depths $[\sigma(\nu)x \ll 1]$, that is always verified in our case, Eq. (3) can be approximated by:

$$T(\nu) \simeq 1 - \sigma(\nu)\,x \, . \tag{4}$$

The cross section $\sigma(\nu)$ must take into account the contribution of the Doppler broadening and the collisional (pressure) broadening. In our measurement conditions other effects like the Dicke narrowing, that happens when the molecular mean free path is comparable to the wavelength of the radiation [19], are not significant and are not taken into account. The right function of the radiation frequency that well describes the absorption coefficient is the Voigt function [20], that is the convolution of the Lorentz and the Gauss curves:

$$f(\nu) = \int\limits_{-\infty}^{+\infty} \frac{\exp\left[-(t - \nu_\circ)^2/\Gamma_{\mathrm{G}}^2 \ln 2\right]}{(t - \nu)^2 + \Gamma_{\mathrm{L}}^2}\,dt \, , \tag{5}$$

where $\nu_\circ$ is the gas resonance frequency and Γ_{L} is the Lorentzian HWHM.

4

Let us assume a laser emission profile varying linearly with the frequency:

$$I_0(\nu) = \bar{I}_0 \, (1 + s \, \nu) \tag{6}$$

where $\bar{I}_0$ is the intensity at $\nu = 0$ and s is the fractional variation per frequency unit. By substituting Eq. (6) in Eq. (2) and taking the second derivative:

$$I''(\nu) = \bar{I}_0(1 + s \, \nu) \, T'' + 2 \, s \, \bar{I}_0 \, T' \,. \tag{7}$$

The apparent displacement of the center depends on the slope s of the profile and on the width Γ_L of the line: by increasing the pressure, the width becomes larger and an apparent shift of the center occurs. This is proportional to the pressure in a way very similar to the real pressure induced shift.

If we assume for simplicity a Lorentz instead of a Voigt shape of the absorption line, Eq. (4) will be:

$$T(\nu) = 1 - S \, x \, \frac{\Gamma_L}{\pi} \, \frac{1}{\nu^2 + \Gamma_L^2} \,. \tag{8}$$

where S is the line strength in $\mathrm{cm}^{-1}/(\mathrm{molecule} \cdot \mathrm{cm}^{-2})$. To get the value of the shift of the maximum $2f$ signal, we expand the second derivative of Eq. (8) around $\nu = 0$:

$$\nu_{\max} = \frac{1}{4} \, \Gamma_L \left(\xi - \frac{5}{16} \xi^3 + ... \right)$$

where $\xi = s \, \Gamma_L$.

Putting $\xi = 0.1$, an acceptable typical value, then $\nu_{\max}/\Gamma_L = \frac{1}{4}\xi \simeq 0.025$; this means that the displacement can be of the same order of magnitude as the pressure induced shift. Thus, if the maximum of the second derivative signal is used to determine the center of the line, this results in an error that is proportional to the width, and hence in an incorrect contribution to the measurement of the pressure-shift coefficient. A refined knowledge of the line-shape parameters is obtained only by fitting the full second derivative signal.

In this work we used Eq. (7) and a nonlinear least-squares fit procedure to extract the line parameters. In particular, to obtain the broadening coefficients we fitted the half-width Γ_L vs pressure by the general expression:

$$\Gamma_L(p) = \gamma_i p_i + \gamma_{self} p_\circ \,, \tag{9}$$

where γ_i is the broadening coefficient related to the i buffer gas, p_i is the buffer gas partial pressure, γ_{self} is the sample gas self-broadening coefficient and $p_\circ$
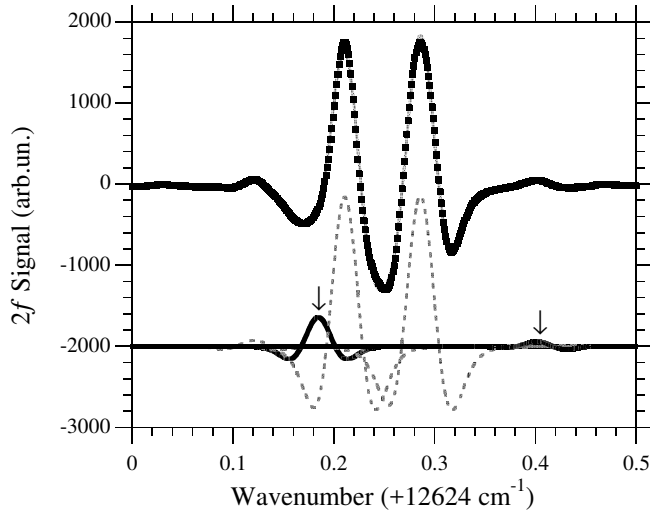
Fig. 3. Ammonia absorption features and their best fit around 12624.25 cm^{-1} obtained by WMS and 2nd harmonic detection at p = 20 Torr and room temperature, with 10 Hz bandwidth. Two new lines have been detected at 12624.18 and 12624.41 cm^{-1}. They are identified among the fitting components by the two arrows.

is the sample gas partial pressure.

3   Experimental results

3.1   Ammonia

In case of ammonia spectroscopy a InGaAlAs SHARP DL Mod. LT025MD that emits 40 mW cw coherent radiation at 785 nm at RT was adopted as the source. The absorption features in this spectral range belong to the overtone $4\nu_1$ (ν_1 : symmetric stretch) and to the combination overtones $2\nu_1 + 2\nu_3$ (ν_3 : asymmetric stretch) of the symmetric top molecule NH$_3$ [21].

An example of spectrum obtained by using the DL spectrometer is shown in Fig. 3, where the second derivative of a small portion of the ammonia overtone band at 792 nm is displayed. The excellent resolving power of the system ($\sim 10^7$) with a "free running" diode can be appreciated: five absorption resonances are observed (12624.12, 12624.18, 12624.21, 12624.29, 12624.41 cm^{-1}), two of which never observed before (12624.18 and 12624.41 cm^{-1}). In the Figure the single peaks obtained by the best fit are shown shifted below the spectrum to better show their positions.

Fitting results for the self-broadening of the ammonia absorption line at
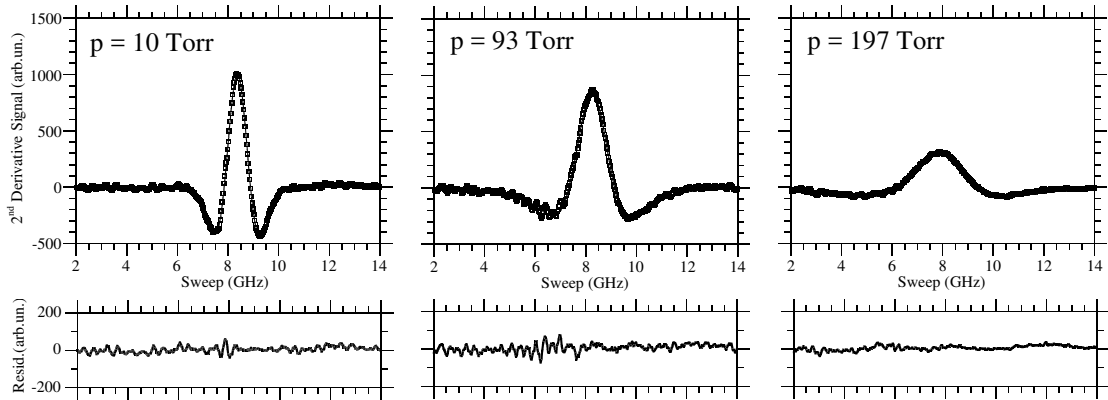
6

Fig. 4. 2nd derivative signals (empty squares) obtained at three ammonia pressures with their best fits (solid lines) and residuals (same units). All the measurements were at room temperature and pertained to the 12682.719 cm^{-1} line. The lock-in amplifier band width was 10 Hz.

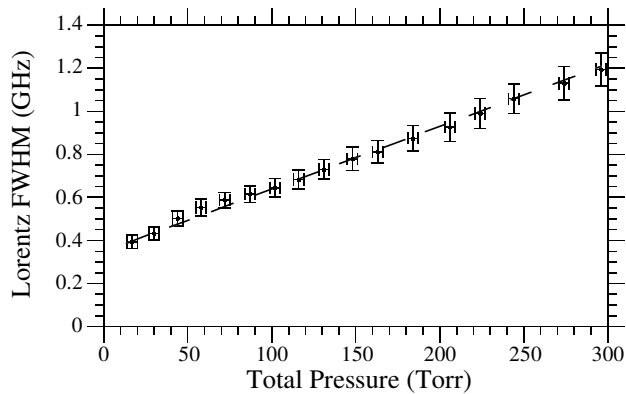Fig. 5. He-broadening for the ammonia line at 12682.719 cm^{-1} (room temperature).

12682.719 cm^{-1} are shown in Fig. 4 for three representative pressures.

Stephen L. Coy and Kevin K. Lehmann [22] gave us their results on these same overtone bands. Starting from their precise line position measurements we have measured line broadening and shifting coefficients for three different buffer gases, which are reported in Tables 1 and 2. All the errors are computed for 3 standard deviations (3σ).

In Fig. 5 the helium pressure-broadened full width at half the maximum (FWHM) for the 12682.719 cm^{-1} ammonia overtone line is shown as an example.

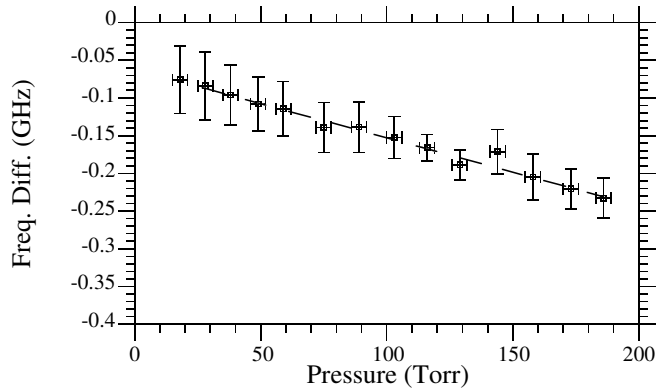In Fig. 6 the self-shifting is plotted as a function of pressure for another over-

7

Fig. 6. Self-shifting of the ammonia line at 12708.449 cm^{-1} line (room temperature).

Table 1
Ammonia collisional-broadening FWHM coefficients (γ) at room temperature (RT).

Wavenumber	γ_{self}	γ_{air}	γ_{H_2}	γ_{He}
(cm^{-1})	(MHz/Torr)	(MHz/Torr)	(MHz/Torr)	(MHz/Torr)
12619.644	28.7 ± 0.4	7.6 ± 0.2	8.8 ± 0.2	3.6 ± 0.5
12627.605	22.8 ± 0.4	7.4 ± 0.1	8.5 ± 0.1	3.6 ± 0.2
12632.919	45 ± 1	8.1 ± 0.2	8.9 ± 0.6	3.3 ± 0.5
12666.263	25.2 ± 0.6	7.6 ± 0.1	7.9 ± 0.3	2.9 ± 0.2
12682.719	24.0 ± 0.1	6.8 ± 0.3	8.6 ± 0.2	2.9 ± 0.1
12686.888	39 ± 1	8.2 ± 0.9	9.6 ± 0.6	3.8 ± 0.3
12699.080	39.9 ± 0.4	6.3 ± 0.3	8.1 ± 0.6	3.6 ± 0.8
12708.499	22.8 ± 0.1	8.3 ± 0.7	8.0 ± 0.2	3.2 ± 0.2
12737.423	46.2 ± 0.1	8.4 ± 0.3	7.7 ± 0.3	3.3 ± 0.3
12739.054	45.4 ± 0.7	7.8 ± 0.1	9.0 ± 0.1	4 ± 1

tone absorption line. Here the frequency shifts do not start from zero, because of a little phase difference between the two lock-in amplifiers used for the measurements.

The complexity of the absorption structure for the symmetric top molecule NH$_3$ in this range permits only a partial assignment of the lines. An attempt has been made by Chao in his work [23] where we could tentatively identify one line ($\nu' = 12737.423$ cm^{-1}) of the R branch with J = 5. By considering the frequency interval between the lines, Chao claims that they belong to one of the four parallel bands expected in this region (792 nm). There is no other

Table 2
Ammonia collisional-shifting coefficients (δ) at RT.

Wavenumber	δ_{self}	δ_{air}	δ_{H_2}	δ_{He}
(cm^{-1})	(MHz/Torr)	(MHz/Torr)	(MHz/Torr)	(MHz/Torr)
12619.644	-4.0 ± 0.2	-1.0 ± 0.2	-0.9 ± 0.4	-0.4 ± 0.1
12627.605	0.7 ± 0.2	-0.5 ± 0.2	-0.6 ± 0.1	0.3 ± 0.1
12632.919	2.0 ± 0.1	-0.3 ± 0.2	-0.5 ± 0.2	0.0 ± 0.1
12666.263	-2.9 ± 0.1	-0.1 ± 0.1	-0.4 ± 0.1	0.1 ± 0.1
12682.719	-0.7 ± 0.2	-0.3 ± 0.2	-0.3 ± 0.2	0.4 ± 0.1
12686.888	0.0 ± 0.5	-0.4 ± 0.3	0.5 ± 0.2	0.8 ± 0.1
12699.080	0.6 ± 0.8	-0.3 ± 0.2	-0.3 ± 0.2	0.0 ± 0.1
12708.499	-0.9 ± 0.1	-0.2 ± 0.2	-0.4 ± 0.3	0.2 ± 0.1
12737.423	2.8 ± 0.1	-0.4 ± 0.1	-0.4 ± 0.1	0.1 ± 0.1
12739.054	0.6 ± 0.6	-0.4 ± 0.1	-0.4 ± 0.1	0.2 ± 0.1

work on broadening coefficients in the VIS and NIR regions. A comparison can be done only with the line broadening measurements performed in the fundamentals vibrational bands ν_2 (11 μm) and ν_4 (6.2 μm) [24–28]. Even if at very different wavelengths, these results are compatible with ours.

3.2 Ethylene

Ethylene is a planar molecule with no permanent dipole moment. The ro-vibrational absorption lines reachable by NIR DLs belong to the third overtone ($4\nu_1$) and are located at about 847 nm. Therefore they are very weak and can be detected only by using very sensitive techniques and long optical path lengths. Monitoring of C_2H_4 is particularly useful in plant physiology as well as for combustion process control.

In this work an AlGaAs Roithner RLT85100G double heterostructure DL and a Herriott type 43 cm multipass cell by SIT S.r.l. were adopted for the purpose. At RT the DL emits single mode 100 mW cw 850 nm coherent radiation at $\sim$ 70 mA. This power is requested to maintain enough power at the exit of the multipass cell. In fact an optical path length of 30 m is produced by 70 reflections on the gold plated mirrors of the cell.

Up to 30 absorption lines have been observed and their position measured

Table 3
Wavelengths (λ) and wavenumbers (ν') list of the observed ethylene absorption lines.

λ @ 294K	ν'	$\sigma_{\max}$	λ @ 294K	ν'	$\sigma_{\max}$
(nm)	(cm^{-1})	(cm^2/molecule)	(nm)	(cm^{-1})	(cm^2/molecule)
844.292	11841.06		846.474	11810.54	4.3×10^{-25}
844.421	11839.25		846.950	11803.90	6.3×10^{-25}
844.607	11836.64	8.1×10^{-25}	847.229	11800.01	
844.881	11832.80	4.9×10^{-25}	847.513	11796.06	
844.945	11831.90	2.2×10^{-25}	847.824	11791.73	
844.993	11831.23		848.078	11788.19	
845.066	11830.21	6.8×10^{-25}	848.353	11784.37	
845.091	11829.86	3.7×10^{-25}	849.752	11764.97	
845.154	11828.98	3.5×10^{-25}	850.721	11751.57	2.0×10^{-25}
845.194	11828.42		850.728	11751.48	7.8×10^{-26}
845.245	11827.70	5.8×10^{-25}	851.085	11746.54	
845.669	11821.77		851.320	11743.31	
845.860	11819.11	4.8×10^{-25}	852.122	11732.26	
845.968	11817.59		852.366	11728.89	
846.231	11813.92	8.7×10^{-25}	852.391	11728.55	

within 0.01 cm^{-1} by comparison with a very precisely known I_2 absorption spectrum [29] and the aid of a I_2 reference cell. Table 3 shows the results with the wavenumbers in vacuum. The listed wavelengths are in air at 294 K and have been deduced by using the index of refraction formula from the work of Edlén [30]. Also the absorption cross section peak values, $\sigma_{\max}$, are shown in the table for the more intense lines. Here the complexity of the structure does not permit an immediate and correct quantum classification of the rovibrational resonances. For these highly excited levels (overtones and higher harmonics), the numerous possible resonances between rovibrational levels, can modify significantly the intensity as well as the position of the expected bands or lines [31].

Despite the very low absorption intensities of these lines, pressure broadening measurements have been attempted on two of the most intense lines at RT. In particular for the 11810.54 cm^{-1} line a higher m has been adopted and the additional instrumental distortion was taken into account through an apparent

Table 4
Ethylene collisional-broadening coefficients at RT.

ν'	γ_{self}	γ_{air}	γ_{H_2}	γ_{He}
(cm^{-1})	(MHz/Torr)	(MHz/Torr)	(MHz/Torr)	(MHz/Torr)
11813.92	9.3 ± 0.2	5.8 ± 0.1	9.8 ± 0.2	5.0 ± 0.1
11810.54	7.4 ± 0.4			
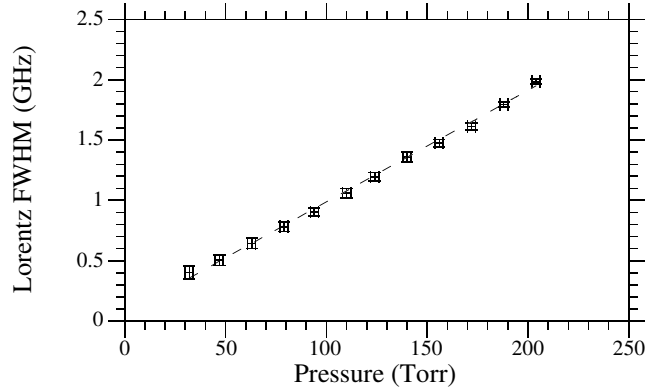
Fig. 7. Self-broadening of the ethylene line at 11813.92 cm^{-1} (room temperature).

Doppler (Gauss) HWHM Γ_{GA} instead of Γ_{G}. The measured coefficients are listed in Table 4.

In the literature there is no collisional broadening measurements at these wavelengths. The only comparison can be done with the works made on the fundamental vibrational bands ν_7 (10.5 μm) [32] and ν_{10} (10.8 μm) [33], where the broadening coefficients are close to ours.

In Fig. 7 the self-broadening measurement result is shown for the 11813.92 cm^{-1} ethylene absorption line.

Adsorption effects on the inner walls of the absorption cell have been observed for both ammonia and ethylene gases. In the literature, ammonia has been reported to stick to the walls of measurement cells [34]. This phenomenon induces an erroneous partial pressure when introducing the buffer gas. The effect can be identified by a non linear behavior of the FWHM of the line when varying the gas pressure, particularly at low pressure. In our case with glass cells at RT the effect was observable only at low He partial pressure when measuring the He-broadening coefficients and it was overcome by ignoring the first few measurement points that were clearly off the expected linear behavior.

11

4   Conclusion

Overtone absorption spectroscopy has been performed on ammonia and ethylene by using a spectrometer based on InGaAlAs and AlGaAs diode lasers. For this purpose the simplest configuration, i.e. *free-running*, along with the wavelength modulation spectroscopy and the second harmonic detection techniques have been adopted. Special care has been put when analyzing the absorption features recorded by this technique. Collisional broadening and shifting coefficients for different perturber gases have been measured at RT for ten ammonia combination overtone absorption lines located in the region 12600–12700 cm^{-1} and also pressure-broadening measurements have been attempted for two ethylene absorption lines. Up to 30 C_2H_4 absorption wavenumber positions around 11800 cm^{-1} have been measured within $0.01 cm^{-1}$ by a comparison with a reference I_2 absorption spectrum. The sensitivity of the diode laser spectrometer is of the order of some tens of ppm per meter of optical path length at atmospheric pressure when applied to the most intense ammonia absorption lines, with a typical time constant of some hundreds of milliseconds. For ethylene the sensitivity is limited to a few parts per thousand per meter, because of the weakness of its 3rd overtone absorption bands.

References

[1] A. Lucchesini, I. Longo, C. Gabbanini, S. Gozzini, L. Moi, Appl. Opt. 32 (1993) 5211–5216.

[2] A. Lucchesini, M. De Rosa, D. Pelliccia, A. Ciucci, C. Gabbanini, S. Gozzini, Appl. Phys. B 63 (1996) 277–282.

[3] G. Blanquet, J. Walrand, and J.-P. Bouanich, J. Mol. Spectrosc. 201 (2000) 56–61.

[4] A. Boschetti, D. Bassi, E. Jacob, S. Iannotta, L. Ricci, M. Scotoni, Appl. Phys. B 74 (2002) 273–278.

[5] D. Romanini, A. Campargue, Chem. Phys. Lett. 254 (1996) 52–58.

[6] J. Wang, M. Maiorov, D.S. Baer, D.Z. Garbuzov, J.C. Connolly, and R.K. Hanson, Appl. Opt. 39 (2000) 5579–5589.

[7] C. Corsi, F. D'Amato, M. De Rosa, and G. Modugno, Eur. Phys. J. D 6 (1999) 327–332.

[8] V. Weldon, J. O'Gorman, P. Phelan, J. Hegarty, T. Tanbun-Ek, Sensors Actuators B 29 (1995) 101–107.

[9] S. Chou, D.S. Baer, and R.K. Hanson, J. Mol. Spectrosc. 196 (1999) 70–76.

[10] C. Corsi, M. Inguscio, S. Chudzynsky, K. Ernst, F. D'Amato, M. De Rosa, Appl. Phys. B 68 (1999) 267–269.

[11] A. Lucchesini, S. Gozzini, C. Gabbanini, Eur. Phys. J. D 8 (2000) 223–226.

[12] A.R. Awtry, J.H. Miller, Appl. Phys. B 75 (2002) 255–260.

[13] A. Lucchesini, S. Gozzini, Eur. Phys. J. D 22 (2003) 209–215.

[14] D.M. Sonnenfroh and M.G. Allen, Appl. Opt. 36 (1997) 7970–7977.

[15] W. Lenth and M. Gehrtz, Appl. Phys. Lett. 47 (1985) 1263–1265.

[16] L. Gianfrani, G. Gagliardi, G. Pesce, A. Sasso, Appl. Phys. B 64 (1997) 487–491.

[17] A. Lucchesini, M. De Rosa, C. Gabbanini, S. Gozzini, Nuovo Cimento D 20 (1998) 253–260.

[18] D.T. Cassidy and J. Reid, Appl. Opt. 21 (1982) 1185–1190.

[19] R.H. Dicke, Phys. Rev. 89 (1953) 472–473.

[20] B.H. Armstrong, J. Quant. Spectrosc. Radiat. Transfer 7 (1967) 61–88.

[21] G. Herzberg, Infrared and Raman Spectra of Polyatomic Molecules, D. Van Nostrand Reinhold Co., New York, p. 296, 1945.

[22] K.K. Lehmann and S.L. Coy, private communication (2002).

[23] S.H. Chao, Phys. Rev. 50 (1936) 27–37.

[24] J.-P. Bouanich, H. Aroui, S. Nouri, A. Picard-Bersellini, J. Mol. Spectrosc. 206 (2001) 104–110.

[25] H. Aroui, M. Broquier, A. Picard-Bersellini, J.-P. Bouanich, M. Chevalier and S. Gherissi, J. Quant. Spectrosc. Radiat. Transfer 60 (2000) 1011–1023.

[26] G. Baldacchini, G. Buffa and O. Tarrini, Nuovo Cimento D13 (1991) 719–733.

[27] G. Baldacchini, G. Buffa, F. D'Amato, O. Tarrini, M. De Rosa, F. Pelagalli, J. Quant. Spectrosc. Radiat. Transfer 67 (2000) 365–374.

[28] M. Dhib, J.-P. Bouanich, H. Aroui and M. Broquier, J. Mol. Spectrosc. 202 (2000) 83–88.

[29] S. Gerstenkorn, J. Verges & J. Chevillard, "Atlas du spectre d'absorption de la molécule d'iode", Lab. Aimé Cotton, Orsay, France, Edition du CNRS, 1982.

[30] Edlén K., Metrologia 2 (1966) 71–80.

[31] T. Platz, W. Demtröder, Chem. Phys. Lett. 294 (1998) 397–405.

[32] J.F. Brannon and P. Varanasi, J. Quant. Spectrosc. Radiat. Transfer 47 (1992) 237–242.

[33] V. Morozhenko, T. Kostiuk, V.E. Blass, T. Hewagama, T.A. Livengood, J. Quant. Spectrosc. Radiat. Transfer 72 (2002) 193–198.

[34] G. Baldacchini, A. Bellatreccia, F. D'Amato, ENEA Report RT/INN/93/07 (1993).